Tropical Journal of Pharmaceutical Research December 2013; 12 (6): 905-912
ISSN: 1596-5996 (print); 1596-9827 (electronic)

Available online at http://www.tjpr.org
http://dx.doi.org/10.4314/tjpr.v12i6.7

Original Research Article

Multivariate Modeling of Cytochrome P450 Enzymes for 4-Aminoquinoline Antimalarial Analogues using Genetic-Algorithms Multiple Linear Regression

Amir Najafi[1]* and Soheil Sobhanardakani[2]
[1]Young Researchers and Elite Club, Hamedan Branch, Islamic Azad University, Hamedan, Iran, [2]Department of the Environment, Hamedan Branch, Islamic Azad University, Hamedan, Iran

For correspondence: **Email: am.najafi@yahoo.com, najafi@iauh.ac.ir; **Tel/Fax:** +98 811 4494143*

Received: 23 September 2013 *Revised accepted: 10 October 2013*

Abstract

Purpose: *To develop QSAR modeling of the inhibition of cytochrome P450s (CYPs) by chloroquine and a new series of 4-aminoquinoline derivatives in order to obtain a set of predictive in-silico models using genetic algorithms-multiple linear regression (GA-MLR) methods.*
Methods: *Austin model 1 (AM1) semi-empirical quantum chemical calculation method was used to find the optimum 3D geometry of the studied molecules. The relevant molecular descriptors were selected by genetic algorithm-based multiple linear regression (GA-MLR) approach. In silico predictive models were generated to predict the inhibition of CYP 2B6, 2C9, 2C19, 2D6, and 3A4 isoforms using a set of descriptors.*
Results: *The results obtained demonstrate that our model is capable of predicting the potential of new drug candidates to inhibit multiple CYP isoforms. A cross-validated Q^2 test and external validation showed that the models were robust. By inspection of R^2_{pred}, and RMSE test sets, it can be seen that the predictive ability of the different CYP models varies considerably.*
Conclusion: *Apart from insights into important molecular properties for CYP inhibition, the findings may also guide further investigations of novel drug candidates that are unlikely to inhibit multiple CYP sub-types.*

Keywords: *Antimalarial, Chloroquine, Cytochrome P450, Genetic algorithm-based multiple linear regression, QSAR.*

Tropical Journal of Pharmaceutical Research is indexed by Science Citation Index (SciSearch), Scopus, International Pharmaceutical Abstract, Chemical Abstracts, Embase, Index Copernicus, EBSCO, African Index Medicus, JournalSeek, Journal Citation Reports/Science Edition, Directory of Open Access Journals (DOAJ), African Journal Online, Bioline International, Open-J-Gate and Pharmacy Abstracts

INTRODUCTION

Malaria is one of the most serious parasitic diseases throughout tropical and subtropical regions, and it remains a major health problem in developing parts of the world [1]. Chloroquine (CQ), a low-cost drug, is widely used as an antimalarial agent. However, the emergence of CQ-resistant malarial parasite strains has prompted the search for alternative strategies to combat the disease.

Application of predictive methods such as quantitative structure-activity relationships (QSAR) and structure-based designs to absorption, distribution, metabolism, elimination and toxicology (ADMET) has become a very active area. Among the ADMET properties, drug metabolism is a key determinant of several important drug processes *in vivo*, such as metabolic stability, drug–drug interactions and drug toxicity [2]. Cytochrome P450 enzymes (CYPs) are an extremely important class of enzymes that are involved in Phase I oxidative

metabolism of structurally diverse chemicals. The human genome contains about 60 P450s, but more than 90 % of all therapeutic drugs are metabolized by five main CYP isoforms: CYP2B6, CYP2C9, CYP2C19, CYP2D6, and CYP3A4 [3]. A considerable number of quantitative structure-activity relationship models have been generated for CYP inhibitors [4-11]. The objective of this study was to demonstrate possibility of obtaining a set of predictive in-silico models for cytochrome P450 2B6, 2C9, 2C19, 2D6, and 3A4 inhibitions, using relatively interpretable descriptors in conjunction with genetic algorithm-based MLR methods.

EXPERIMENTAL

Ensemble ADME data and molecular descriptors

We used a series of 4-aminoquinoline antimalarial compounds with experimentally-determined ADME properties [12]. Based on the results of this research group [12], antimalarial compounds that are effective against drug-resistant strains of P. falciparum by varying the chemical substitutions around the heterocyclic ring and the basic amine side chain of the popular antimalarial drug chloroquine have been developed [13,14]. Several of these novel antimalarial compounds have been screened for improved leads based on the evaluated ADMET properties [12]. Figure 1 depicts the structures of the compounds used in this study. The panel includes a small number of CQ analogues with altered substitutions on the quinoline ring, although the majority of the compounds in the panel contain substitutions of the alkyl groups attached to the basic nitrogen position on the aminoalkyl side chain.

The inhibitory activity of the test compounds at two concentrations, 1 and 10 μM, was tested on various CYPs in pooled human liver microsomes (HLMs) including CYP2B6, CYP2C9, CYP2C19, CYP2D6, and CYP3A4. In this assay, HLMs were incubated with a test compound and a cocktail of specific P450 substrates for each enzyme. The known major metabolites of the substrates were subsequently quantified by LC/MS/MS to compute the percentage of inhibition due to the test compound in comparison to the percentage in non-drug-treated controls. As a rule of the thumb, enzyme activity levels of <70 % of the level observed for the untreated controls were considered to be significant inhibition. The majority of the compounds inhibited the CYP2D6 enzyme. Table 1 shows the data for 21 chloroquine analogues and their percent inhibition.

The molecular structures of all the chloroquine derivatives were built with Hyperchem (Version 7, HyperCube, Inc.) software. AM1 semi-empirical calculation was used to optimize the 3D geometry of the molecules. The Polak-Ribier algorithm with root mean squares gradient 0.1 kcal/mol was selected for optimization. By using DRAGON [15], we derived a total of 1481 1D, 2D, and 3D molecular descriptors from the 3D structure of each compound.

The list and meaning of the molecular descriptors is provided by the DRAGON package, and the calculation procedure is explained in detail, with related literature references, in the Handbook of Molecular Descriptors [16].

MLR modeling procedure

Multiple Linear Regression (MLR) which demonstrates great ease of implementation along with the interpretability of resulting equations was the statistical method of choice for building the QSAR model. The forward-stepping variant of Multiple Linear Regression (MLR) was utilized, starting with the selection of a single variable which contributes most to the model based on its highest F-statistics or lowest p-value. At each step, MLR alters the model from the previous step by adding predictor variables and terminating the search when a statistically significant model has been obtained [17,18]. Genetic algorithm (GA) search was carried out exploring MLR models. The GA used was the same as that previously used [19,20].

The Selected Descriptors

The majority of the selected descriptors in our GA-MLR modeling are composite descriptors, which can be divided into five groups: GETAWAY, 3D-MoRSE, RDF, WHIM and 2D autocorrelations descriptors. Table 2(a) and 2(b) depicts the names and meanings of the molecular descriptors used in this work.

Validation of the models

A good fit was assessed based on the determination squared correlation coefficients (R^2), adjusted determination coefficient (R^2_{adj}), standard deviation (s), root-mean-square error (RMSE), Fisher's statistic (F) and number of variables. The robustness and predictive ability of the model was evaluated by Q^2 based on leave-one-out (LOO) cross-validation. This procedure consists of removing one data point from the training set and constructing the model only on the basis of the remaining training data

and then testing on the removed point. In order to make more realistic validation of the predictive power of the models, external validation was also performed. For that purpose, six chloroquine derivatives (3, 6, 8, 15, 18 and 19) were selected from 21 compounds at random to construct the external test set, and the remaining 15 chloroquine derivatives comprised the training set that was employed to calibrate the QSAR models.

Ring substitution analogs

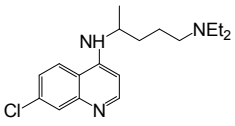

(1)

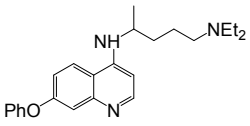

(2)

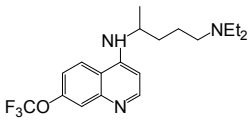

(3)

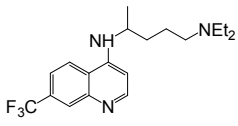

(4)

Side chain substitution analogs

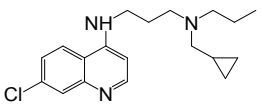

(5)

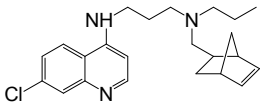

(6)

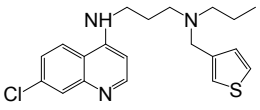

(7)

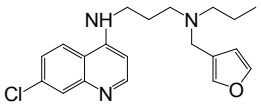

(8)

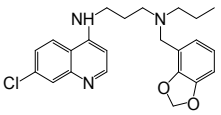

(9)

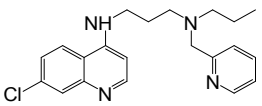

(10)

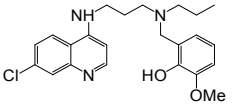

(11)

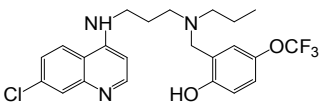

(12)

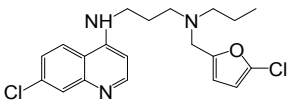

(13)

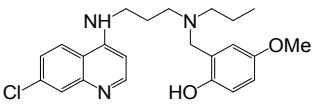

(14)

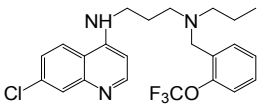

(15)

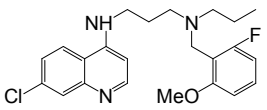

(16)

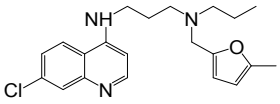

(17)

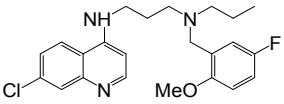

(18)

Secondary amine side chain analogs

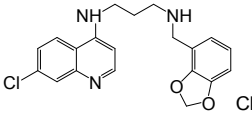

(19)

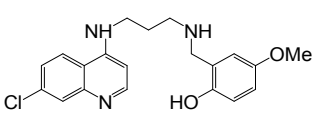

(20)

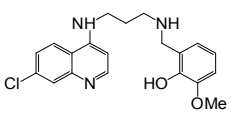

(21)

Figure 1: Chemical structures of 4-aminoquinoline analogues used in this study

Table 1: Inhibition of Cytochrome P450 isoforms by the test compounds at concentrations of 1 and 10 µM

Compound	CYP inhibition (metabolite produced as % of control)											
	CYP2B6		CYP2C9		CYP2C19		CYP2D6		CYP3A4[a]		CYP3A4[b]	
	1 µM	*10 µM*	*1 µM*	*10 µM*	*1 µM*	*10 µM*	*1 µM*	*10 µM*	*1 µM*	*10 µM*	*1 µM*	*10 µM*
1	112	134	114	128	113	111	99	90	105	110	102	106
2	119	118	118	115	120	126	101	72	114	125	102	125
3	99	109	105	145	109	115	81	57	107	120	108	120
4	97	121	103	126	93	107	94	94	94	111	96	113
5	95	112	102	121	107	115	83	63	101	108	103	105
6	108	107	109	73	104	114	61	13	89	30	76	26
7	98	117	98	96	104	120	55	22	103	92	102	82
8	111	108	113	104	97	108	60	15	101	94	99	89
9	114	115	119	122	117	136	23	8	109	96	107	84
10	104	117	107	108	108	110	85	49	108	85	102	89
11	96	113	97	106	103	119	56	15	103	85	94	57
12	98	114	96	79	108	107	98	10	97	63	80	39
13	96	100	98	79	90	102	61	13	90	69	87	75
14	108	128	107	128	110	113	94	87	105	102	102	88
15	98	113	93	63	107	115	64	17	101	68	92	53
16	106	109	104	100	104	127	73	20	100	82	99	87
17	94	107	85	46	101	106	53	11	97	57	89	46
18	99	110	102	93	94	123	79	4	89	66	84	62
19	94	112	98	115	104	121	76	29	99	66	96	70
20	103	98	102	102	100	119	91	56	101	102	103	90
21	105	105	108	108	113	122	96	69	106	108	108	97

[a] *Data expressed as % metabolism of known substrates for each isoform compared to control. The known substrates are as follows: CYP2B6 (bupropion, 25 µM), CYP2C9 (diclofenac, 10 µM), CYP2C19 (mephenytoin, 50 µM), CYP2D6 (bufuralol, 10 µM), CYP3A4a (midazolam, 4 µM), and CYP3A4b (testosterone, 50 µM). Values of < 70% are considered to be significant inhibition.*

Table 2(a): Brief description of GETAWAY and 3D-MoRSE molecular descriptors used in the different modeling approaches

GETAWAY	
H3u	H autocorrelation of lag 3 / unweighted
HTm	H total index / weighted by atomic masses
HATS7e	leverage-weighted autocorrelation of lag 7 / weighted by ase
RTu	R total index / unweighted
$R1u_+$	R maximal autocorrelation of lag 1 / unweighted
R4m	R autocorrelation of lag 4 / weighted by atomic masses
$R5m_+$	R maximal autocorrelation of lag 5 / weighted by atomic masses
$R7m_+$	R maximal autocorrelation of lag 7 / weighted by atomic masses
R8v	R autocorrelation of lag 8 / weighted by avv
$R5v_+$	R maximal autocorrelation of lag 5 / weighted by avv
$R8v_+$	R maximal autocorrelation of lag 8 / weighted by avv
$R5e_+$	R maximal autocorrelation of lag 5 / weighted by ase
$R7e_+$	R maximal autocorrelation of lag 7 / weighted by ase
$R8e_+$	R maximal autocorrelation of lag 8 / weighted by ase
3D-MoRSE	
Mor12u	3D-MoRSE - signal 12 / unweighted
Mor16u	3D-MoRSE - signal 16 / unweighted
Mor22u	3D-MoRSE - signal 22 / unweighted
Mor23u	3D-MoRSE - signal 23 / unweighted
Mor02m	3D-MoRSE - signal 02 / weighted by atomic masses
Mor04m	3D-MoRSE - signal 04 / weighted by atomic masses
Mor12m	3D-MoRSE - signal 12 / weighted by atomic masses
Mor28m	3D-MoRSE - signal 28 / weighted by atomic masses
Mor03v	3D-MoRSE - signal 03 / weighted by avv
Mor06v	3D-MoRSE - signal 06 / weighted by avv
Mor11v	3D-MoRSE - signal 11 / weighted by avv
Mor24v	3D-MoRSE - signal 24 / weighted by avv

Table 2(b): Brief description of RDF, WHIM and 2D autocorrelations molecular descriptors used in the different modeling approaches

RDF	
RDF060u	Radial Distribution Function - 6.0 / unweighted
RDF140u	Radial Distribution Function - 14.0 / unweighted
RDF055m	Radial Distribution Function - 5.5 / weighted by atomic masses
RDF095m	Radial Distribution Function - 9.5 / weighted by atomic masses
RDF155m	Radial Distribution Function - 15.5 / weighted by atomic masses
RDF030v	Radial Distribution Function - 3.0 / weighted by avv
RDF060v	Radial Distribution Function - 6.0 / weighted by avv
RDF065v	Radial Distribution Function - 6.5 / weighted by avv
WHIM	
G2v	2st component symmetry directional WHIM index / weighted by avv
G3v	3st component symmetry directional WHIM index / weighted by avv
P1e	1st component shape directional WHIM index / weighted by ase
P2e	2st component shape directional WHIM index / weighted by ase
Du	D total accessibility index / unweighted
2D autocorrelations	
MATS3m	Moran autocorrelation - lag 3 / weighted by atomic masses
MATS2p	Moran autocorrelation - lag 2 / weighted by atomic polarizabilities
GATS4m	Geary autocorrelation - lag 4 / weighted by atomic masses

Avv: atomic van der Waals volumes, ase: atomic Sanderson electronegativities

RESULTS

QSAR models for human cytochrome P450 Inhibitors (CYPs)

Inhibition of CYPs can lead to drug-drug interactions and therefore it is considered important to evaluate potential drug candidates for CYP-inhibitory activities. Percent inhibition of CYP activities by the chloroquine analogues was calculated from the ratios of the activities of inhibited to control samples. Incubation conditions (enzyme concentration and substrates) for each of the inhibition assays are summarized in Table 1.

This section describes the pharmacophore models that have been constructed for various P450s by using the QSAR techniques. A genetic algorithm was used to remove descriptors irrelevant to the prediction of CYP450 inhibitors. The retained descriptors from this process were used for representing the compounds studied in this work. Summaries of the relevant datasets employed for generating the QSARs relating the various molecular descriptors to the CYP-inhibitory potencies of Chloroquine analogues used in this work are shown in Table 3 (a), 3(b).

Table 3(a): Multivariate Linear regression models and statistical parameters for 2B6, 2C9 and 2C19 P450 Inhibitors

CYP[a]	Equation	R^2	R^2_{adj}	RMSE	F	Q^2
2B6 (1μM)	3.137(0.092) - 0.591(0.046) R4m - 5.761 (0.555) G2v + 0.077(0.013) Mor11v + 0.393(0.060) MATS2p - 0.215(0.044) $R1u_+$ + 0.452(0.143) $R5m_+$	0.95	0.93	0.01	45.98	0.88
2B6 (10μM)	2.083(0.046) + 0.148(0.011) Mor22u + 10.149(2.239) GATS4m - 0.007(0.001) RDF095m - 0.006(0.001) Mor02m - 0.168(0.052) P2e	0.93	0.91	0.01	40.69	0.85
2C9 (1μM)	3.227(0.135) - 0.012(0.001) HTm - 7.055(0.849) G2v + 0.041(0.006) Mor04m - 0.044(0.010) Mor12m + 1.015(0.375) $R8v_+$	0.90	0.87	0.01	27.76	0.83
2C9 (10μM)	12.436(1.344) + 0.095(0.008) Mor03v - 11.280(1.346) MATS3m - 0.346(0.052) Mor28m + 6.527(1.444) G3v + 1.284(0.322) $R7m_+$	0.95	0.94	0.03	60.06	0.90
2C19 (1μM)	3.096(0.105) - 5.977(0.701) G2v - 2.086(0.326) $R8v_+$ - 0.585(0.076) HATS7e + 2.254(0.429) $R5v_+$ - 0.071(0.029) Mor24v	0.91	0.88	0.01	31.76	0.84
2C19 (10μM)	2.046(0.011) - 0.011(0.001) RDF055m + 0.003(0.000) RDF060u + 0.027(0.005) Mor12u + 0.006(0.001) RDF030v	0.93	0.92	0.01	56.06	0.88

Table 3(b): Multivariate Linear regression models and statistical parameters for 2D6 and 3A4 P450 Inhibitors

CYP[a]	Equation	R^2	R^2_{adj}	RMSE	F	Q^2
2D6 (1μM)	3.968(0.408) - 0.054(0.005) RDF060v - 0.241(0.030) Mor04m + 0.146(0.039) Mor06v - 3.302(0.615) $R5e_+$ - 0.061(0.016) RTu	0.93	0.90	0.04	38.41	0.80
2D6 (10μM)	2.953(0.159) - 7.512(0.637) R8v - 0.741(0.100) Mor16u - 0.155(0.020) RDF155m + 0.041(0.009) RDF140u	0.95	0.93	0.09	97.86	0.91
3A4[a] (1μM)	2.402(0.112) - 0.396(0.051) $R7e_+$ - 0.057(0.012) Mor23u - 1.419(0.252) $R8v_+$ - 0.002(0.001) RDF055m - 2.338(0.673) G2v	0.93	0.90	0.01	39.09	0.86
3A4[a] (10μM)	-1.430(0.310) + 1.186(0.139) P1e + 11.353(1.804) G3v + 2.187(0.362) Du - 2.580(0.548) $R8e_+$	0.94	0.92	0.03	61.06	0.89
3A4[b] (1μM)	2.697(0.193) - 1.591(0.180) $R8e_+$ 2.858(0.594) G3v - 3.668(0.829) G2v - 0.114(0.010) H3u -0.004(0.001) Mor02m	0.94	0.92	0.01	45.20	0.88
3A4[b] (10μM)	1.411(0.391) - 2.085(0.292) P2e - 1.466(0.306) $R7e_+$ - 0.025(0.006) RDF065v + 8.195(2.499) G3v	0.92	0.90	0.05	46.31	0.86

The known substrates are as follows: CYP3A4a (midazolam 4 μM), and CYP3A4b (testosterone 50 μM).

The predictive power of the model was determined by using LOO cross-validation and by the use of a test set of 6 structurally and biologically diverse chloroquine analogues excluded from the model creation. A cross-validated Q^2, obtained as a result of this analysis, served as a quantitative measure of the predictive ability of the final QSAR models. The Q^2 value is a statistical indication of how well a model can predict the activity of members left out of the model formation. The training and test sets and statistical parameters for each CYP model are also presented in Table 4. The quality of the fit of the training set of a specific model was measured by its R^2. However, a most important measure is the prediction quality; the R^2_{pred} and RMSE of the test set give a more realistic guide to the predictive power of the P450 CYP models (Table 4). Graphical representation of the performance of each approach in adjusting and predicting CYP inhibition data is also presented in Figure 2.

Table 4. Evaluation of the prediction ability of the MLR models in the external validation set for Different P450 Inhibitors

CYP[a]	Training set				Test set	
	R^2	*R^2_{adj}*	*RMSE*	*F*	*R^2_{pred}*	*RMSE*
2B6 (1μM)	0.98	0.96	0.03	19.51	0.74	0.01
2B6 (10μM)	0.96	0.94	0.01	43.13	0.39	0.02
2C9 (1μM)	0.95	0.92	0.01	34.90	0.61	0.02
2C9 (10μM)	0.97	0.95	0.02	58.67	0.91	0.04
2C19 (1μM)	0.95	0.93	0.01	36.67	0.84	0.02
2C19 (10μM)	0.96	0.94	0.01	55.82	0.78	0.01
2D6 (1μM)	0.93	0.89	0.04	24.37	0.82	0.03
2D6 (10μM)	0.95	0.93	0.08	50.51	0.92	0.13
3A4[a] (1μM)	0.90	0.85	0.01	16.39	0.96	0.01
3A4[a] (10μM)	0.92	0.89	0.03	28.60	0.97	0.07
3A4[b] (1μM)	0.94	0.91	0.01	29.12	0.92	0.02
3A4[b] 10μM)	0.87	0.81	0.05	16.32	0.89	0.07

DISCUSSION

The GETAWAY (Geometry, Topology, and Atom Weights AssemblY) descriptors try to match the 3D molecular geometry provided by the molecular influence matrix and atom relatedness by topology with chemical information by using various atomic weighting schemes (unit weights, mass, polarizability, electronegativity). 3D-MoRSE descriptors, which are representations of the 3D structure of a molecule and encode features such as molecular weight, van der Waals volume, electronegativities, and polarizabilities. The radial distribution function (RDF) descriptors are based on the distance distribution of the compounds. The RDF

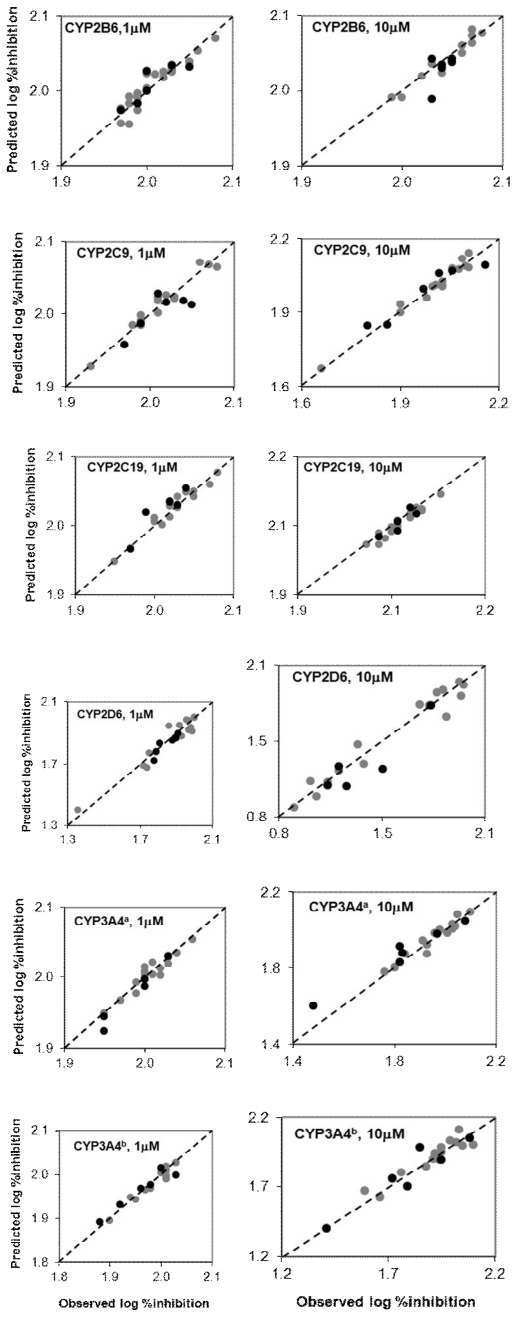

Figure 4: Predicted versus Observed CYP enzyme inhibitory activities values expressed as log percent inhibitory. The LOO cross-validation of compounds are represented as grey dots and the test set as black do

descriptors of a molecule of n atoms can be interpreted as the probability distribution of finding an atom in a spherical volume of radius R. RDF descriptors provide information about bond lengths, ring types, planar and nonplanar systems, atom types, and molecular weight and have been used for pharmacokinetic studies. WHIM descriptors are based on statistical indices calculated on the projections of atoms along principal axes. The aim is to capture 3D information regarding size, shape, symmetry and atom distributions with respect to invariant reference frames. 2D autocorrelations descriptors, in general explain how the considered property is distributed along the topological structure. Three spatial autocorrelation vectors including unweighted and weighted Moran, Geary and Broto–Moreau autocorrelation vectors were calculated. The physicochemical property considered in atomic masses (m), atomic van der Waals volumes (v), atomic Sanderson electronegativities (e), and atomic polarizabilities (p) as weighting properties [16].

A cross-validated Q^2 test showed that the models were robust (Table 3(a), 3(b)). Also external validation yielded statistically significant and accurate predictions of pIC50 values for the majority of the CYP enzyme isoforms. By inspection of the R^2_{pred}, and RMSE test sets, it can be seen that the predictive ability of the different CYP models varies considerably. A weak correlation (R^2_{pred} = 0.39) was found between experimental and predicted 2B6 (at 10µM) data (Table 4). However, exclusion of one outlier (compound 8) resulted in a fairly good correlation (R^2_{pred} = 0.79), with the descriptors. Although the RMSE of the 2B6 model is lower at 0.03, suggesting this model predicts with lower error, this is a result of the test set observations having the smallest standard deviation. The RMSE of 2B6 model approaches the standard deviation of the observed data (i.e. a random prediction). We can conclude that the presence of most descriptors reveals the important role of size, shape, flexibility, atomic atomic van der Waals volume and atomic masses weighted terms of molecules on ligand- P450 isoenzyme interaction.

CONCLUSION

A quantitative structure–activity relationship (QSAR) study was applied to the series of 4-aminoquinoline antimalarial compounds. For each strain, statistically significant models were obtained using the GA-based MLR method. These models may be considered as mathematical equations for the prediction of antimalarial activities of the compounds structurally similar to those used in this study. In silico models for CYP 2B6, 2C9, 2C19, 2D6 and 3A4 inhibition was undertaken using multiple linear regression method and a set of descriptors. The CYP models range from moderate to highly predictive and thus could prove useful in assessing the P450 liability of molecules for a particular isoform.

REFERENCES

1. World Health Organization; World malaria report, 2009. Available from: http://www.who.int/malaria/publications/atoz/9789241563901/en/index.html.
2. Li AP. Screening for human ADME/Tox drug properties in drug discovery. Drug Discov Today 2001; 6: 357-366.
3. Arimoto R, Computational models for predicting interactions with cytochrome P450. Enzyme Curr Top Med Chem 2006; 6: 1609-1618.
4. Hutzler JM, Walker GS, Wienkers LC. Inhibition of cytochrome P450 2D6: structure-activity studies using a series of quinidine and quinine analogues. Chem Res Toxicol 2003; 16: 450-459.
5. Kemp CA, Flanagan JU, van Eldrik AJ, Marechal JD, Wolf CR, Roberts GCK, Paine MJI, Sutcliffe MJ. Validation of model of cytochrome P450 2D6: an in silico tool for predicting metabolism and inhibition. J Med Chem 2004; 47: 5340-5346.
6. Crivori P, Poggesi I. Predictive model for identifying potential CYP2D6 inhibitors. Pharmacol Toxicol 2005; 96: 251-253.
7. Yap CW, Chen YZ. Prediction of cytochrome P450 3A4, 2D6, and 2C9 inhibitors and substrates by using support vector machines. J Chem Inf Model 2005; 45: 982-992.
8. Gleeson MP, Davis, AM, Chohan KK, Paine SW, Boyer S, Gavaghan CL, Arnby CH, Kankkonen C, Albertson N. Generation of in-silico cytochrome P450 1A2, 2C9, 2C19, 2D6, and 3A4 inhibition QSAR models. J Comput Aided Mol Des 2007; 21: 559-573.
9. Kontijevskis A, Komorowski, J, Wikberg, JES. Generalized proteochemometric model of multiple cytochrome P450 enzymes and their inhibitors. J Chem Inf Model 2008; 48: 1840-1850.
10. Roy K, Roy PP. Exploring QSAR and QAAR for inhibitors of cytochrome P450 2A6 and 2A5 enzymes using GFA and G/PLS techniques. Eur J Med Chem 2009; 44: 1941-1951.
11. Veselovsky AV, Sobolev BN, Zharkova MS, Archakov AI. Computer-based substrate specificity prediction for cytochrome P450. Biochem (Moscow) B Biomed Chem 2010; 4: 75-81.
12. Ray S, Madrid PB, Catz P, LeValley SE, Furniss MJ, Rausch LL, Guy RK, DeRisi JL, Iyer LV, Green CE, Mirsalis JC. Development of a new generation of 4-Aminoquinoline antimalarial compounds using predictive pharmacokinetic and toxicology models. J Med Chem 2010; 53: 3685-3695.
13. Madrid PB, Liou AP, DeRisi JL, Guy RK. Incorporation of an intramolecular hydrogen-bonding motif in the side chain of 4-aminoquinolines enhances activity against drug-resistant P. Falciparum. J Med Chem 2006; 49: 4535-4543.
14. Madrid PB, Sherrill J, Liou AP, Weisman JL, Derisi JL, Guy RK. Synthesis of ring-substituted 4-aminoquinolines and evaluation of their antimalarial activities. Bioorg Med Chem Lett 2005; 15: 1015-1018.
15. Dragon, Talete. Italian chemometrics Inc.; c1993- 2010 [cited 2003 Mar 8]. Available from: http://www.talete.mi.it
16. Todeschini R, Consonni, V. Handbook of Molecular Descriptors, London: Wiley- VCH; 2000.
17. Darlington RB. Regression and Linear Models,: New York: McGraw-Hill; 1990.
18. Najafi A, Ardakani SS. 2D autocorrelation modelling of the anti-HIV HEPT analogues using multiple linear regression approaches. Mol Simulat 2011; 37: 72-83.
19. Najafi A, Ardakani SS, Marjani M. QSAR analysis of the anticonvulsant activity of some benzylacetamides based on Genetic-MLR. Trop J Pharm Res 2011; 10(4) : 483-490.
20. Ghavami R, Najafi A, Sajadi M, Djanati F. Chemometrics-assisted spectrophotometric methods for simultaneous determination and complexation study of Fe(III), Al(III) and V(V) with morin in micellar media. J Mol Graphics Modell 2008; 70: 824-834.